JOURNAL OF PHYSICAL ORGANIC CHEMISTRY
J. Phys. Org. Chem. 2005; **18:** 217–226
Published online 27 July 2004 in Wiley InterScience (www.interscience.wiley.com). DOI: 10.1002/poc.839

Boron trifluoride activated enaminocarbonyl compounds: the influence of intermolecular interactions on the *ab initio* determination of structures and vibrational spectra†

Joachim Nikolai,[1] Gerhard Maas[1] and Gerhard Taubmann[2]*

[1]Abteilung Organische Chemie I, Universität Ulm, Albert-Einstein-Allee 11, 89081 Ulm, Germany
[2]Abteilung Theoretische Chemie, Universität Ulm, Albert-Einstein-Allee 11, 89081 Ulm, Germany

Received 9 February 2004; revised 20 April 2004; accepted 4 May 2004

ABSTRACT: The structures of the BF_3–enaminoaldehyde adducts **3a**, **b** have been determined by quantum-chemical calculations employing Hartree-Fock, Møller-Plesset and density functional methods. The length of the coordinative B—O bond ranges between 1.59 and 1.62 Å. The BSSE-free energy of the B—O bond ranges between −14.7 and −16.9 kcal/mol. Taking into account hydrogen bonds and dispersion forces between two molecules of **3a**, **b** in the dimeric structure **4** reduces the B—O bond length significantly (B—O: 1.52–1.57 Å) thereby reproducing the B—O bond length found in the x-ray structure of **1** (B—O: 1.49 Å) with much better accuracy. Using the calculated IR and Raman spectra of the dimers **4** as reference, the B—O band in the experimental spectra can be assigned. Our approach seems to be of value in discussions comparing structural features gained from gas phase *ab initio* calculations and solid state x-ray structures involving strong dipolar structures which allow for various intermolecular interactions.

Supplementary electronic material for this paper is available in Wiley Interscience at http://www.interscience.wiley.com/jpages/0894-3230/suppmat/

KEYWORDS: enaminocarbonyl compounds; Lewis acids; vibrational spectra; quantum chemical calculations

INTRODUCTION

As a method of choice for enhancing the reactivity of carbonyl compounds, complexation of the carbonyl oxygen atom with Lewis acids has found broad application in organic synthesis.[1,2] Various model adducts obtained from boron-based Lewis acids and carbonyl compounds, such as benzaldehyde-BF_3,[3] methacrolein-BF_3,[4] dimethyl formamide and BX_3 (X = F, Cl, Br, I) or B-bromocatecholborane[5] have been isolated and characterized by x-ray analysis. Also the structures of complexes of PhC(=O)R (R = H, Me, OEt, N*i*Pr$_2$) with $B(C_6F_5)_3$ have been investigated.[6]

Recently, the preparation and spectroscopic characterization was reported of acyclic 1:1 complexes formed between enaminocarbonyl compounds and BF_3 as well as BPh_3.[7] This study also presents the x-ray crystal structures of complexes **1** and **2** (Fig. 1). The results confirmed O-coordination of the Lewis acid and revealed a nearly planar zigzag configuration of the B—O—C_1—C_2—C_3—N chain along with an expressed bond length equalization in the complexed enaminoaldehyde moiety. Restricted Hartree-Fock (RHF) and density functional calculations (DFT) employing the B3LYP functional for **2** gave results in good agreement with the crystallographic data for the complexed enaminocarbonyl compound.[7]

For **2**, the experimentally determined B—O bond length (x-ray: 1.597 Å) and the computed values (RHF/6–31G(d): 1.637 Å, B3LYP/6–31G(d): 1.623 Å) differed by ≤0.04 Å. For **1**, however, the computed B—O bond lengths (RHF/6–31+G(d): 1.563 Å, B3LYP/6–31+G(d): 1.591 Å) were too long by 0.07—0.1 Å with respect to the experimentally determined value (x-ray: 1.496 Å). DFT calculations on the structure of benzaldehyde–BF_3 gave a B—O distance of 1.67 Å (x-ray:[3] 1.59 Å) and for methacrolein–BF_3 1.69 Å (x-ray:[4] 1.58 Å).[7] Again, the calculated bond distances are longer by 0.08 and 0.11 Å. It was assumed that intermolecular interactions which are known to have a detectable influence on the internal coordinates of molecules in crystals may be at the origin of the pronounced differences between the experimentally determined B—O bond lengths and the calculated values.[7,8] Our reasoning was supported by the observation of various intermolecular (B)F···H—C contacts in

**Correspondence to:* G. Taubmann, Abteilung Theoretische Chemie, Universität Ulm, Albert-Einstein-Allee 11, 89081 Ulm, Germany.
E-mail: gerhard.taubmann@chemie.uni-ulm.de
†Dedicated to Professor Heinz-Dieter Rudolph on occasion of his 80th birthday.

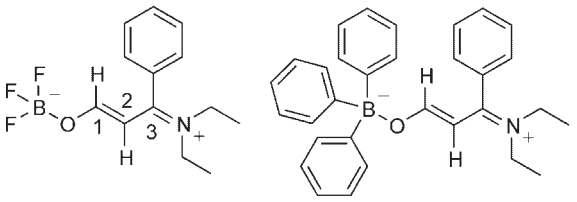

1 2

Figure 1. Adducts of (*E*)-3-diethylamino-3-phenyl-2-propenol with BF_3(1) and BPh_3(2)

the crystal structure of the BF_3 adduct **1**. In the structure of the BPh_3 adduct **2** no intermolecular contacts were detected.[7] For the structures of benzaldehyde–BF_3 and methacrolein–BF_3, hydrogen–fluorine contacts similar to those observed in **1** were not reported.[3,4] Beside an MNDO calculation for the benzaldehyde–BF_3 adduct reporting a B—O distance of 1.607 Å (x-ray: 1.59 Å)[3] there are two reports describing *ab initio* calculations for model compounds of the general structure $R^1R^2C{=}O{\cdot}H_2BF$ ($R^1 = H$, alkyl; $R^2 = H$, alkyl, alkynyl) but providing no values for the B—O bond length.[9,10] The latter studies focused on the stabilization of the Lewis acid/base adducts through anomeric effects and hydrogen bonding between the RCHO group and the boron moiety. The results served as an explanation for the remarkable stereochemical control which is achieved in reactions involving the activation of carbonyl compounds with chiral boranes.[11–13]

Using a computationally more amenable model system for **1** (*vide infra*: molecule **3**, Fig. 2), the results of our studies are presented which are intended to give a quantitative description of the effects influencing the B—O bond in **1** if the possibility of hydrogen bonding and dispersion effects between two neighbouring molecules is taken into account. The basis set superposition error (BSSE) corrected bond strength and bond length for the dative B—O bond are reported, as well as the BSSE free interaction energy found in a dimer constructed with our model BF_3 adduct allowing for hydrogen bonds and van der Waals forces.

COMPUTATIONAL METHODS

Restricted Hartree-Fock (RHF), density functional theory (DFT, using the B3LYP functional) and second order Møller-Plesset perturbation theory (MP2) methods implemented in the Gaussian 98 program package were used for geometry optimizations.[14] MP2 calculations were carried out with full electron correlation. Standard convergence criteria as implemented in the modelling program were applied using geometry constraints as indicated in Tables 2–4. All calculated minimum structures on the potential energy surface are characterized by having only positive eigenvalues of the Hessian matrix. Population analysis was done with the program package

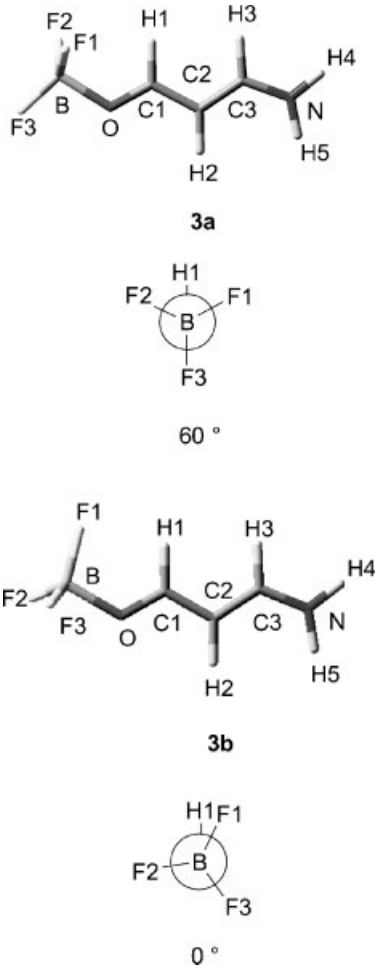

Figure 2. 3a: HF and MP2 structures with staggered conformation. **3b**: B3LYP structure with eclipsed conformation (see text for details)

NBO 3.1[15] implemented in Gaussian 98. Basis set superposition error free bonding energies,[16–19] geometries and frequencies[19,20] were computed using the counterpoise correction as implemented in Gaussian 98.[14] Dimers, constructed from two molecules of a model 'monomeric' BF_3–enaminocarbonyl adduct (*vide infra*) were used to probe the influence of intermolecular hydrogen bonds and dispersion forces on the B—O bond length. To create the dimeric starting structures, a small Fortran 77 program was written which, after reading in a Gaussian input file containing twice the identical structure of the monomer given in cartesian coordinates, rotated the second monomer around the Eulerian angles[21] θ, ϕ and Ψ first and then translated it along the cartesian coordinates. The output was written as Gaussian input file allowing the structure of the dimer to be examined using GaussView 2.08. These well defined dimeric structures were optimized using Gaussian 98. Calculated IR and Raman data were extracted from the Gaussian output with the help of a Fortran 77 program which allowed for empirical frequency scaling (RHF/6–31+G(d): 0.90, MP2/6–31+G (d): 0.94, B3LYP/6–31+G(d): 0.96)[22] and assignment of

a Gaussian line shape (half width used: 40 cm^{-1}) to the IR and Raman transitions. Its output was used to draw spectra using Origin 6.1®.

EXPERIMENTAL METHODS

The IR spectrum of **1** in a KBr pellet was recorded on a Bruker Vector 22 FT-IR spectrophotometer at room temperature employing a HeNe laser working at 632.82 nm. The Raman spectrum was taken from a sample of **1** enclosed in an argon flushed Raman tube using a LabRam instrument at room temperature employing a HeNe laser working at 632.82 nm (focal length 300 mm, grid 1800). For unknown reasons, C—H bands in the Raman spectrum appear to be considerably weaker than expected from the calculations (cf. Figure 10c, d).

RESULTS AND DISCUSSION

Bonding in enaminocarbonyl–BF_3 complexes

In order to ascertain the previously obtained RHF and DFT results for **1** and **2** (*vide supra*)[7] and to discuss the observed bond length patterns observed in **1** including MP2 calculations and more flexible basis sets, a model for **1** was constructed which retained only the BF_3–enaminocarbonyl backbone, having replaced the phenyl ring at C3 and the ethyl substituents at the nitrogen atom by hydrogen atoms (**3a**, **b**, Fig. 2). Since almost free rotation around the B—O bond was found, a conformational scan in steps of 10° for a rotation of 60° around a fictive B—C_1 bond was performed, allowing all other geometry parameters to relax fully. The rotation around a hypothetical B—C_1 bond instead of the B—O bond was chosen for an easy definition of a torsion angle between the B—F bonds and the C_1—H_1 bond. A staggered all–*trans*, C_S symmetric conformation (**3a**, Fig. 2), designated as 60° in the Newman projections of Fig. 2 was found as minimum from RHF and MP2 calculations. The observed rotational barriers about the hypothetical B—C_1 bond are 0.08 kcal/mol [RHF/6–31+G(d)], 0.03 kcal/mol [RHF/6–31++G(d,p)], 0.22 kcal/mol [MP2/6–31+G(d)] and 0.19 kcal/mol [MP2/6–31++G(d,p)]. On the other hand, B3LYP calculations employing the same basis sets reversed the picture and showed the eclipsed conformation **3b**, designated as 0°, to be the minimum conformation. Here, the rotation barrier was found to be 0.24 kcal/mol [B3LYP/6–31+G(d)] and 0.30 kcal/mol [B3LYP/6–31++G(d,p)]. The s–*trans* conformation at the C_1—C_2 bond is in agreement with the calculated structure of the acrolein–BH_3 adduct.[23]

Bond lengths and angles for **3a**, **b** listed in Table 1—including planarization of the enamine nitrogen atom—indicate a slight polarization of the enaminocarbonyl moiety towards an iminium enolate structure, thereby reproducing the results of a previous B3LYP/6–31+G(d) optimization of the full structure of **1**.[7] Once again the structures for **3a**, **b** fail fully to reproduce the experimentally observed bonding structure: the calculated B—O bond lengths are significantly longer than in the x-ray structure of **1**.[7] Nevertheless, the results obtained for **3a**, **b** indicate that the substituents at C1 and C3 have no effect on the bonding pattern of the B—O—C3—N chain and **3a**, **b** may be used for further calculations intended to study influences on the B—O bond length. Table 1 also provides the counterpoise corrected bonding energy of the B—O bond which is computed as follows:[16–19] ΔE_{el} is the electronic interaction energy between the BF_3 and the enaminoaldehyde calculated by subtracting from the total energy of the complex the energies of the uncomplexed BF_3 and enaminoaldehyde having the same geometry as in the complex using the complexes' full basis set (i.e. placing ghost atoms in the positions of the enaminoaldehyde and BF_3, respectively). ΔE_{relax} is defined as the energy needed to distort BF_3 and the enaminoaldehyde from the geometry of the free molecules to the geometry they have in the complex. The BSSE-free energy of the B—O bond is defined as $E_{B—O} = \Delta E_{el} + \Delta E_{\text{relax}}(BF_3) + \Delta E_{\text{relax}}(\text{enamino})$. The BSSE is obtained by subtracting from E_{total} the energies of the uncomplexed enaminoaldehyde, the uncomplexed BF_3 and the energy of the B—O bond ($E_{\text{B—O}}$), using the basis sets of the uncomplexed molecules for enaminoaldehyde and BF_3. To correct the potential energy surface for the BSSE between the BF_3 and the enaminoaldehyde moiety in adducts **3a**, **b**, a counterpoise corrected optimization and frequency calculation was performed on the RHF/6–31+G(d), B3LYP/6–31+G(d) and MP2/6–31+G(d) structures of **3a**, **b**.[14,20] For these structures, the interaction energies were then re-calculated[24] (Table 2).

Experimental gas phase data for complexes between boron based Lewis acids and carbonyl compounds are not available. (A literature search in the MOGADOC[25] database for compounds of general structure $R^1R^2C{=}O\cdots B(XYZ)$ gave no hits.) However, comparison of calculated bond lengths (Tables 1 and 2) with gas phase data available from electron diffraction experiments for BF_3 complexes with amines and ethers indicates that the B—O bond calculated for **3a**, **b** is at the lower edge of the reported values: e.g. r_g(B—N) = 1.674(4) Å for trimethylamine–BF_3 and r_g(B—O) = 1.75(2) Å for dimethylether–BF_3.[26,27] Inclusion of electron correlation at both the DFT and the MP2 level of theory lengthen the B—O bond with respect to RHF calculations, although it is known that RHF calculations already give too long bond lengths for dative bonds.[28] At the DFT level of theory, the B—O bond energy is found to be largest, whereas at the MP2 level the lowest energies are found. BSSE effects on the total energy, the boron–oxygen bond length and bond energy are most significant for the MP2 calculations (Tables 1 and 2), e.g. the B—O bond is lengthened by 0.038 Å due to the counterpoise correction. For all three

Table 1. Selected bond lengths (Å) and angles (°) for RHF, MP2 and DFT optimized structures of **3a** and **3b**; see Figure 2 for atom numbering

Compound	**3a**				**3b**	
Level of theory	RHF/6–31+G(d)	RHF/6–31++G(d,p)	MP2/6–31+G(d)	MP2/6–31++G(d,p)	B3YLP/6–31+G(d)	B3LYP/6–31++G(d,p)
B—O[a]	1.590(9)	1.590(7)	1.620(1)	1.623(5)	1.619(5)	1.619(3)
O—C1[a]	1.233(0)	1.233(1)	1.263(4)	1.262(2)	1.259(4)	1.259(5)
C1—C2[a]	1.409(9)	1.410(0)	1.409(1)	1.409(9)	1.411(6)	1.411(6)
C2—C3[a]	1.360(1)	1.359(7)	1.370(9)	1.369(7)	1.373(0)	1.372(6)
C3—N[a]	1.329(9)	1.329(3)	1.341(0)	1.341(2)	1.342(4)	1.342(2)
C3—N—H5	121.3(5)	121.1(2)	121.3(2)	121.1(9)	121.4(9)	121.3(0)
C3—N—H4	121.3(4)	121.1(9)	121.4(1)	121.1(6)	121.4(1)	121.3(0)
H4—N—H5	117.3(0)	117.6(7)	117.2(6)	117.6(5)	117.0(9)	117.3(9)
E_{total}[b]	−569.045 671	−569.059 481	−570.408 710	−571.902 725	−571.902 578	−571.914 344
ZPE[b,c]	0.102	0.101	0.095	0.095	0.095	0.095
NImag[d]	0	0	0	0	0	0
Point group	C_S	C_S	C_S	C_S	C_S	C_S
ΔE_{el}[e] [kcal/mol]	−46.02	−46.06	−40.79	−39.92	−42.75	−42.78
$\Delta E_{rel}(BF_3)$[f] [kcal/mol]	28.70	28.71	24.24	23.86	24.06	24.06
ΔE_{rel}(enamino)[g] [kcal/mol]	2.65	2.58	2.33	2.35	1.87	1.90
$E_{B—O}$[h] [kcal/mol]	−14.67	−14.77	−14.23	−13.72	−16.82	−16.82
BSSE[i] [kcal/mol]	2.13	2.13	6.73	6.69	1.45	1.45

[a] Bond lengths of **1** in the solid:[7] B—O: 1.496(3), O—C1: 1.307(2), C1—C2: 1.357(2), C2—C3: 1.422(3), C3—N: 1.315(2) Å.
[b] Hartree per molecule.
[c] *ZPE*: zero point energy in harmonic approximation.
[d] *NImag*: number of imaginary frequencies.
[e] ΔE_{el}: electronic interaction energy between BF_3 and enaminaldehyde (see text for details).
[f] ΔE_{rel}: (BF_3): relaxation energy for BF_3 fragment (see text for details).
[g] ΔE_{rel} (enamino): relaxation energy for enaminoaldehyde fragment (see text for details).
[h] $E_{B—O}$: BSSE free energy of B—O bond (see text for details)
[i] *BSSE*: basis set superposition error.

Table 2. Selected bond lengths (Å) and angles (°) for RHF, MP2 and DFT optimized structures of **3a** and **3b** including the BSSE during the optimization; see Figure 2 for atom numbering

Compound	**3a**		**3b**
Level of theory	RHF/6–31+G(d)	MP2/6–31+G(d)	B3YLP/6–31+G(d)
B—O[a]	1.596(1)	1.658(2)	1.625(2)
O—C1[a]	1.233(4)	1.261(4)	1.258(8)
C1—C2[a]	1.409(7)	1.410(4)	1.411(9)
C2—C3[a]	1.360(3)	1.369(9)	1.373(2)
C3—N[a]	1.329(9)	1.342(1)	1.342(4)
C3—N—H5	121.3(4)	121.4(1)	121.4(1)
C3—N—H4	121.3(4)	121.3(2)	121.5(0)
H4—N—H5	117.3(0)	117.2(6)	117.0(8)
E_{total}[b]	−569.045 657	−570.408 446	−571.902 492
ZPE[b,c]	0.101	0.095	0.095
NImag[d]	0	0	0
Point group	C_S	C_S	C_S
ΔE_{el}[e] [kcal/mol]	−46.43	−39.52	−42.90
$\Delta E_{rel}(BF_3)$[f] [kcal/mol]	29.07	23.01	24.21
ΔE_{rel}(enamino)[g] [kcal/mol]	2.67	1.72	1.86
$E_{B—O}$[h] [kcal/mol]	−14.68	−14.79	−16.83
BSSE[i] [kcal/mol]	2.11	6.40	1.44

For footnotes, see Table 1.

methods the B—O bond length is increased by the counterpoise correction as expected. Our results are in agreement with other studies examining the interaction energies and bond lengths in various other adducts, emphasizing the effect of the BSSE on MP2 calculations.[24] At all levels of theory, the relaxation energy (ΔE_{relax}) for the deformation of the BF_3 moiety from the trigonal-planar geometry of free BF_3 to the pyramidal geometry in **3a**, **b** gives the largest contribution to the relaxation energy term (Table 1).

To obtain an estimate of the influence of hydrogen bonds and dispersion forces on the structure of the BF_3–enaminocarbonyl adduct **1**, and especially on its coordinative B—O bond, model dimer **4** was constructed from two units of **3**. Since there are two molecules oriented in an antiparallel manner in the unit cell of **1**,[7] an antiparallel orientation of the monomers in the model dimer was chosen. Starting from the same initial structure, RHF, DFT and MP2 optimizations employing the small 3–21G basis set were carried out in a first step. Neglecting minimal differences in their geometry (Table 3), the B3LYP and MP2 calculations ended up in the same minimum structure. Although the RHF and the DFT and MP2 structures differ considerably in their geometrical details (Fig. 3), both lead to C_2 symmetric, slightly bent structures for the initially C_S symmetric BF_3–enaminocarbonyl monomers. The planes containing the B—O—C_1—C_2—C_3—N chain of the monomer units are nearly perpendicular to each other. Bending of the monomer unit occurs towards its twin, indicating intermolecular interactions between the BF_3 moiety of one monomer and the iminium moiety in the other monomer. No attempts were made to find other structures of dimer **4**, because the primarily interest was in the effects of dimer formation on the structure of the monomer units and especially on changes concerning the B—O bond. Structures with a considerably higher symmetry (e.g. C_{2h} with a centre of inversion) than found in the solid state structures would also oversimplify the calculated IR and Raman spectra due to the rule of mutual exclusion.

Re-optimization of the dimeric structures obtained with the 3–21G basis set with the more flexible 6–31+G(d) basis set changed the geometries of the RHF and B3LYP structures only slightly (Fig. 4). A pronounced change in the relative orientation of the monomers was observed for the MP2/6–31+G(d) dimer (Fig. 5): the BF_3–enaminoaldehyde units are found in a nearly parallel orientation to each other which is in distinct contrast to the perpendicular orientation in the MP2/3–21G structure.

Table 3. Selected bond lengths (Å) and angles (°) for RHF/3–21G, MP2/3–21G and B3LYP/3–21G optimized structures of dimer **4**; see Figure 3 for atom numbering

Level of theory	RHF/3–21G	MP2/3–21G	B3YLP/3–21G
B—O[a]	1.519(6)	1.566(7)	1.551(1)
O—C1[a]	1.287(2)	1.313(2)	1.306(5)
C1—C2[a]	1.370(6)	1.388(4)	1.382(0)
C2—C3[a]	1.384(2)	1.400(3)	1.394(2)
C3—N[a]	1.306(8)	1.326(7)	1.321(9)
C3—N—H5	122.9(4)	122.3(9)	122.5(4)
C3—N—H4	117.8(3)	116.3(2)	116.1(5)
H4—N—H5	118.6(3)	120.2(1)	119.9(9)
E_{total}[b]	−1131.975 689	−1133.785 196	−1137.617 185
ZPE[b,c]	0.212	0.200	0.198
NImag[d]	0	0	0
Point group	C_2	C_2	C_2

For footnotes, see Table 1.

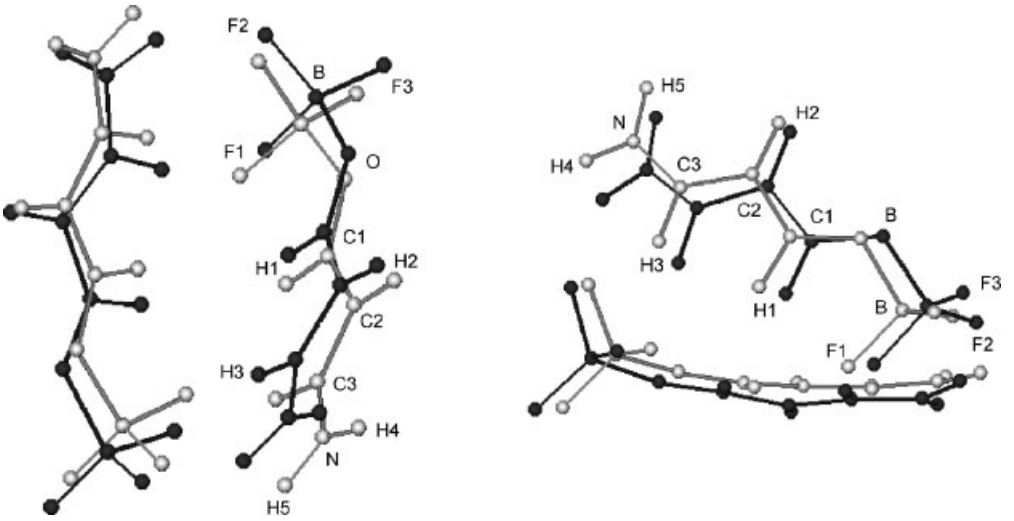

Figure 3. RHF/3–21G optimized structure (black) and B3LYP resp. MP2/3–21G optimized structure of **4** (grey). (a) top view, (b) side view (see text for details)

Although it is known that HF and DFT methods do not reproduce interaction energies which are purely due to dispersion forces,[30] there are examples in which HF and B3LYP calculations were successfully applied in the computational treatment of complexes such as BF_3–methylcyclopropane[31] or HCN–BF_3.[32] The latter study used a dimeric structure in an approach similar to ours to assess the influence of intermolecular forces on the coordinative N—B bond in HCN–BF_3. The strong changes observed in the MP2 structure of dimer **4** when going from the 'hard' 3–21G valence shell basis set to the more flexible 6–31+G(d) may be interpreted in terms of supplementary dispersion effects between the two BF_3–enaminoaldehyde units which can be reproduced by the inclusion of diffuse functions. These are interactions which are only taken into account by correlation methods like at least MP2.[30] An increased basis set in the RHF and B3LYP calculations does not change the structures significantly; the effects seen in the bonding patterns of the monomers at these levels of theory seem to be mainly due to hydrogen bonding which is known to be reproduced fairly well by HF and B3LYP calculations.[30,31] Focusing on the change in the B—O bond lengths in the dimeric structures (Tables 3 and 4), it is seen that there is virtually no change in the bond lengths for the B3LYP and MP2 structures when going from the 3–21G basis set to 6–31+G(d). Comparing the results for the 6–31+G(d) basis set from Table 1 and Table 4 for the monomers and the dimers, respectively, the influence of intermolecular

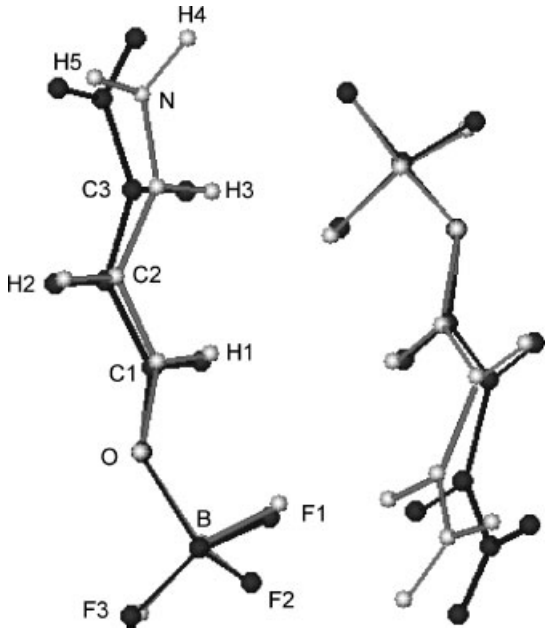

Figure 4. RHF/3–21G (grey) and RHF/6–31+G(d) (black) optimized structures of **4**. Similar structures are found from B3LYP calculations with the same basis sets

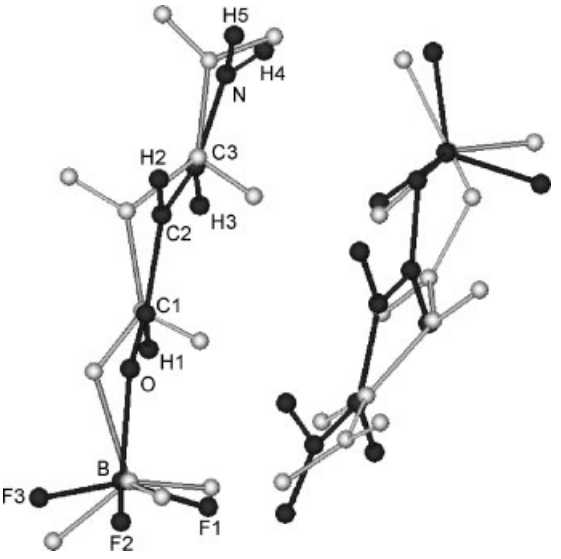

Figure 5. MP2/3–21G (grey) and MP2/6–31+G(d) (black) optimized structures of **4**

Table 4. Selected bond lengths (Å) and angles (°) for RHF/6–31+G(d), MP2/6–31+G(d) and B3LYP/6–31+G(d) optimized structures of dimer **4**; see Figures 4 and 5 for atom numbering

Level of theory	RHF/6–31+G(d)	MP2/6–31+G(d)	B3YLP/6–31+G(d)
B—O[a]	1.531(3)	1.560(0)	1.557(7)
O—C1[a]	1.251(6)	1.285(0)	1.276(7)
C1—C2[a]	1.390(2)	1.387(9)	1.394(0)
C2—C3[a]	1.377(7)	1.387(5)	1.389(8)
C3—N[a]	1.316(1)	1.322(8)	1.326(5)
C3—N—H5	121.6(7)	120.6(9)	121.5(5)
C3—N—H4	119.7(1)	119.9(0)	118.3(6)
H4—N—H5	117.4(8)	115.4(8)	117.8(1)
E_{total}[b]	−1138.124 741	−1140.864 782	−1143.834 423
ZPE[b,c]	0.206	0.194	0.192
NImag[d]	0	0	0
Point group	C_2	C_2	C_2
ΔE_{el}[e] [kcal/mol]	−24.22	−26.89	−26.28
ΔE_{rel}(monomers)[f] [kcal/mol]	4.33	5.54	6.10
E(dimer)[g] [kcal/mol]	−19.89	−21.35	−20.17
BSSE[h][kcal/mol]	1.21	8.35	1.10

[a–d] see Table 1.
[e] ΔE_{el}: electronic interaction energy between monomers.
[f] ΔE_{rel}(monomers): relaxation energy of monomers.
[g] *E*(dimer): BSSE free interaction energy between monomers in the dimer structure.
[h] *BSSE*: basis set superposition error.

forces on the structure of the BF_3-adducts becomes obvious: the B—O bond lengths become shorter by about 0.06 Å at all levels of theory. Compared with the crystal structure of **1**[7] this reduces the difference from the experimentally determined B—O bond length to +0.03 Å (RHF) and +0.06 Å (MP2, B3LYP). For the monomers (Table 1) the difference amounts to 0.13 Å in the worst case. As a consequence of the stronger interaction between the Lewis acid and the carbonyl group, the polarization of the enaminoaldehyde moiety towards an iminium-enolate becomes much more pronounced in the dimers than in the monomers: especially the lengthening of the O—C_1 bond (RHF: +0.018 Å, B3LYP: +0.017 Å, MP2: +0.022 Å) and the C_2—C_3 bond (RHF: +0.17 Å, B3LYP: +0.16 Å, MP2: +0.17 Å) as well as the shortening of the C_3—N amine/iminium bond (RHF: −0.013 Å, B3LYP: −0.016 Å, MP2: −0.019 Å) clearly indicate, that for the chemically correct description of the experimentally found condensed phase structure of **1**, the influence of neighbouring molecules has to be taken into account. Interaction energies between the monomers rise in the order RHF < B3LYP < MP2 (Table 4). Once again, the BSSE is found to be most prominent for the MP2 calculations (*vide supra*).

Table 5 provides the dipole moments and the atomic charges found by a natural population analysis[32] for the monomers and the dimers. The intermolecular interactions due to hydrogen bonds in the dimers are seen by

Table 5. Natural population analysis for monomers and dimers; see Figures 2, 4, 5 for atom numbering

Level of theory	RHF/6–31+G(d)		MP2/6–31+G(d)		B3YLP/6–31+G(d)	
Structure	Monomer (**3a**)	Dimer (**4**)	Monomer (**3a**)	Dimer (**4**)	Monomer (**3b**)	Dimer (**4**)
C1	0.557	0.518	0.372	0.340	0.372	0.344
H1	0.192	0.210	0.210	0.219	0.213	0.211
C2	−0.527	−0.543	−0.434	−0.440	−0.432	−0.437
H2	0.254	0.249	0.262	0.257	0.258	0.257
C3	0.231	0.277	0.102	0.142	0.103	0.130
H3	0.231	0.264	0.245	0.263	0.245	0.264
N	−0.859	−0.835	−0.804	−0.743	−0.793	−0.757
H4	0.440	0.453	0.446	0.469	0.442	0.472
H5	0.437	0.431	0.440	0.439	0.436	0.429
O	−0.700	−0.738	−0.564	−0.638	−0.581	−0.625
B	1.565	1.562	1.397	1.392	1.417	1.419
F1	−0.612	−0.630	−0.563	−0.565	−0.572	−0.580
F2	−0.612	−0.621	−0.563	−0.583	−0.554	−0.580
F3	−0.594	−0.597	−0.544	−0.551	−0.554	−0.546
Dipole moment [Debye]	13.60	6.43	13.34	5.22	13.68	6.43

comparing the atomic charges of atoms F1 and F2 in one molecule and H3* and H4* in its twin molecule. As negative charge is built up on the fluorine atoms and positive charge accumulates on the neighbouring hydrogen atoms, the dipolar structures of the BF_3–enaminocarbonyl adducts are strengthened and contribute to the stronger polarization of the enaminoaldehyde units in the dimers. The decrease of negative charge on the iminium-nitrogen atom in the dimer relative to the corresponding monomer and the more negatively charged oxygen atom illustrate this concept and underline the analysis made on the basis of bond lengths in the monomers and dimers (*vide supra*).However, the *overall* dipole moment of the dimers is decreased, as is expected for the head-to-tail arrangement of the BF_3–enaminoaldehyde adducts, and directed along the C_2 axis. It is worth noting that the second hydrogen atom (H5) of the amino group and the third fluorine atom (F3) of the BF_3 group are considerably less positively (H5) or negatively (F3) charged than the atoms F1, F2 and H4 which are in close contact to atoms of the other monomer. This effect is less pronounced for F3 and in the MP2 calculations.

Raman and IR spectra of enaminocarbonyl–BF_3 complexes

Having shown the importance of including intermolecular forces in the quantum chemical description of boron–enaminocarbonyl complexes in order to obtain good agreement with experimentally determined solid state bond lengths, the changes in structure observed between monomers and dimers were examined to see if they were reflected in the calculated IR and Raman spectra. Of especial interest was whether the deviations seen between the calculated spectra for the isolated molecule **1** and the experimental data were similar to the differences between the calculated spectra of monomers and dimers of model compound **3**. The discussion is focused on the intense and unequivocally assigned bands of the B—O, C═O and C═N valence vibrations for the calculated structures **1**[7] and **3**. Based on the insights gained from the calculations, the experimental spectra of **1** were examined and a tentative assignment of the corresponding bands in these spectra is given. It should be noted for further discussion that the vibration denoted as 'C═N band' actually is a valence vibration involving three atoms, i.e. C2—C3—N, in which the nuclear motion is located mainly on C3 in a bond stretching/compressing motion with C3 bouncing back and forth between C2 and N.

Figures 6, 7 and 8 show the calculated IR and Raman spectra for the monomers and dimers. As is seen in connection with Table 6 in all cases the B—O vibration experiences a hypsochromic shift in the dimers. Referring back to the BSSE free optimized structures for monomers (**3a**, **b**; Table 2), the B—O vibration in the monomers is shifted to slightly lower wavenumbers due to the BSSE

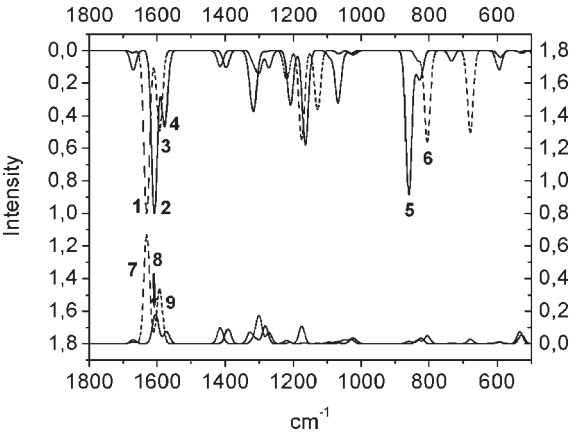

Figure 6. Calculated IR and Raman spectra [RHF/6–31+G(d)]. Top: IR; bottom Raman. Dashed line: monomer **3a**; straight line: dimer **4**. The intensities are given in arbitrary units. The labels refer to Table 6

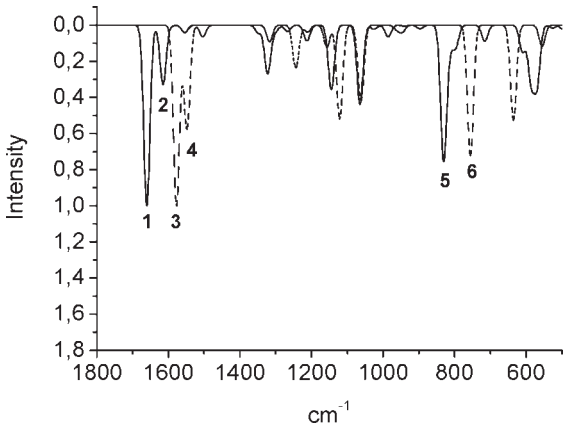

Figure 7. Calculated IR spectra [MP2/6–31+G(d)]. Dashed line: monomer **3a**; straight line: dimer **4**. Raman spectrum not calculated. The intensities are given in arbitrary units. The labels refer to Table 6

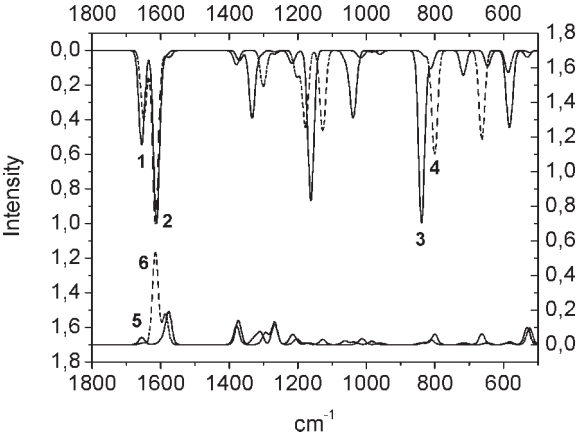

Figure 8. Calculated IR and Raman spectra [B3LYP/6–31+G(d)]. Top: IR; bottom Raman. Dashed line: monomer **3b**; straight line: dimer **4**. The intensities are given in arbitrary units. The labels refer to Table 6

Table 6. Assignment of some harmonic frequencies obtained from calculations with the 6–31+G(d) basis set. Only clearly located vibrations are assigned

Description[a]	RHF (Fig. 6)[b]	MP2 (Fig. 7)[b]	B3LYP (Fig. 8)[b]
C═O (**3**)	1630.96 (1, 7)	1616.60 (4)	1615.58 (6)
C═O (**4**)	1608.24 (2, 8)	1649.62 (2)	1612.25 (2)
Δ(C═O)	−22.72	+33.02	−3.33
C═N (**3**)	1592.55 (3, 9)	1647.20 (3)	1649.67 (1)
C═N (**4**)	1578.13 (4)	1660.62 (1)	1655.53 (5)
Δ(C═N)	−14.42	+13.42	+5.86
B—O (**3**)	805.34 (5)	788.96 (6)	800.76 (4)
B—O (**4**)	860.27 (6)	830.56 (5)	839.28 (3)
Δ(B—O)	+54.93	+41.60	+38.52

[a] Given are the frequencies of the monomer (**3**:**3a** for RHF and MP2, **3b** for B3LYP), of the dimer (**4**), and their difference $\Delta = \nu$ (dimer)$-\nu$ (monomer).
[b] The band n° in the figures are given in parenthesis. The frequencies are given in cm^{-1}.

with the MP2 calculation experiencing the strongest effect: RHF/6–31+G(d): $-2.33\,cm^{-1}$, MP2/6–31+G(d): $-8.92\,cm^{-1}$, B3LYP/6–31+G(d): $-1.57\,cm^{-1}$. All calculated Raman spectra show no bands in the region of the B—O and B—F absorptions. Although changes in bond lengths in the dimers relative to the monomers have the same direction for the C1—O, C2—C3 and C3—N bonds at all levels of theory, this is not uniformly reflected in the calculated vibrational spectra for the C═O and C═N bands: The MP2 calculation yields the expected hypsochromic shifts, whereas the RHF calculation gives a bathochromic shift for these bands in the dimer (Table 6). For the MP2 and B3LYP IR spectra, the hypsochromic shift of the C═N band inverts the order of the C═O and C═N vibration, predicting the C═N vibration at higher wavenumbers than the C═O absorption. The intensity for the C═O vibration is predicted to be more intensive than the C═N band for the RHF and B3LYP calculations. At the MP2 level the intensities for these bands are reversed (Fig. 9).

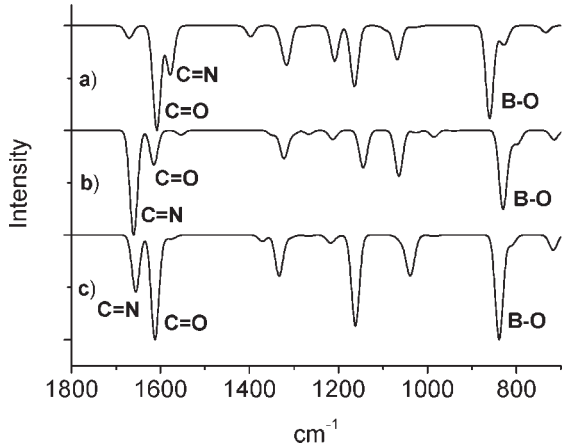

Figure 9. Extension comparing calculated IR spectra for dimers **4**: (a) RHF/6–31+G(d); (b) MP2/6–31+G(d); (c) B3LYP/6–31+G(d)

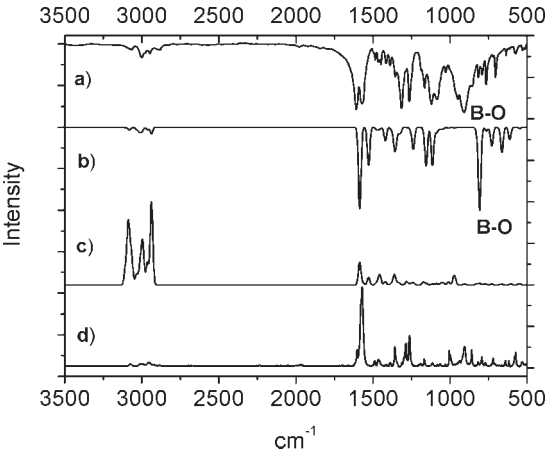

Figure 10. (a) Experimental IR for **1**; (b) calculated IR for **1** [B3LYP/6–31+G(d)]; (c) calculated Raman for **1** [B3LYP/6–31+G(d)]; (d) experimental Raman for **1**. For unknown reasons, C—H bands in the Raman spectrum appear to be considerably weaker than expected from the calculations

The experimental spectra for **1**, together with the calculated spectra for a B3LYP/6–31+G(d) optimization[7] of the isolated, complete structure of **1** are shown in Fig. 10. The calculated IR and Raman spectra [Fig. 10, spectra (b) and (c)] predict an intense C═O band at $1584.7\,cm^{-1}$ and a weaker C═N absorption at $1528.1\,cm^{-1}$. The B—O band is predicted to be at $807.6\,cm^{-1}$. Contrasting this, the experimental band is found at $907.1\,cm^{-1}$ (Fig. 10a). A value much closer to the experimental wavenumber for the B—O vibration is achieved when dimeric structures as discussed above are considered (see Table 6). As predicted by the calculations there is no absorbance in the range of the B—O vibrations in the Raman spectrum. Though there can be no doubt of the correct assignment of the B—O band, it has to be noted that the calculated spectra for the dimers still predict the B—O band at lower frequencies than found in the experiment (RHF: $860.27\,cm^{-1}$; B3LYP: $839.28\,cm^{-1}$; MP2: $830.56\,cm^{-1}$). Contrary to the case of the B—O band, the results of the calculations on the C═O and the C═N bands deviate considerably for the different methods as outlined above. Therefore, an assignment of these vibrations is not given. Further experiments, e.g. using isotopic substitution, are beyond the scope of this work.

CONCLUSION

Taking into account hydrogen bonds and dispersion forces between the molecules of the BF_3–enaminoaldehyde adduct **3a**, **b** in a dimeric structure similar to the situation found in a crystal structure analysis of **1**,[7] quantum-chemical calculations predict a more polarized iminium-enolate structure of the enaminoaldehyde in the BF_3 adduct and a significantly reduced B—O bond length compared with the monomeric structure. Calculations

using only monomers do not reproduce the x-ray structure with similar accuracy. Using the calculated IR and Raman spectra of the dimers as reference, the B—O band in the experimental spectra can be assigned. In accordance with the observation that the B—O bond length in the solid state of **1** is distinctly shorter than in the calculated gas-phase structure of monomeric **3a**, **b**, the experimental B—O vibration of **1** exhibits a pronounced hypsochromic shift compared with the calculated (gas-phase) value for **3**. Overall, our approach could be of value in discussions comparing structural features gained from gas phase *ab initio* calculations and solid state x-ray structures. It is an example of how intermolecular forces may influence the bond geometries.

Acknowledgement

The authors wish to thank Alexander Legant (Jobin Yvon, Bensheim) for recording the Raman spectrum of **1** and Franz Zdichafsky and Professor Dr A. Ruoff (both at Ulm) for valuable discussion. The calculations were made possible in the frame of the Center of Excellence for Computational Chemistry, a collaborative project between the University of Ulm and Sun Microsystems (http://www.uni-ulm.de/coe). We thank Thomas Nau at the Universitätsrechenzentrum Ulm for local implementation of Gaussian 98 and for generous allocation of CPU time. We also thank Dr Jürgen Vogt (Ulm) for a literature search using the MOGADOC database. J. N. thanks the Land Baden-Württemberg for a postgraduate fellowship.

REFERENCES

1. Shambayati S, Schreiber SL. In *Comprehensive Organic Synthesis*, vol. 1, chapter 1.10, Trost BM, Fleming I (eds). Pergamon Press: Oxford, 1991.
2. Yamamoto H (ed). *Lewis Acid Reagents—A Practical Approach.* Oxford University Press: New York, 1999.
3. Reetz MT, Hüllmann M, Massa W, Berger S, Rademacher P, Heymanns P. *J. Am. Chem. Soc.* 1986; **108**: 2405–2408.
4. Corey EJ, Loh TP, Sarshar S, Azimioara M. *Tetrahedron Lett.* 1992; **35**: 6945–6948.
5. Corey EJ, Rohde JJ, Fischer A, Azimioara MD. *Tetrahedron Lett.* 1997; **38**: 33–36.
6. Parks DJ, Piers WE, Parvez M, Atencio R, Zaworotko MJ. *Organometallics* 1998; **17**: 1369–1377.
7. Nikolai J, Taubmann G, Maas G. *Z. Naturforsch.* 2003; **58b**: 217–225.
8. Hargittai M, Hargittai I. *Int. J. Quantum Chem.* 1992; **44**: 1057–1067.
9. Goodman JM. *Tetrahedron Lett.* 1992; **33**: 7219–7222.
10. Mackey MD, Goodman JM. *Chem. Commun.* 1997; **24**: 2383–2384.
11. Corey EJ, Rohde JJ. *Tetrahedron Lett.* 1997; **38**: 37–40.
12. Corey EJ, Lee TW. *Chem. Commun.* 2001; **15**: 1321–1329.
13. Corey EJ. *Angew. Chem.* 2002; **114**: 1724–1741; *Angew. Chem. Int. Ed.* 2002; **41**: 1650–1667.
14. (a) Frisch MJ, Trucks GW, Schlegel HB, Scuseria GE, Robb MA, Cheeseman JR, Zakrzewski VG, Montgomery Jr. JA, Stratmann RE, Burant JC, Dapprich S, Millam JM, Daniels AD, Kudin KN, Strain MC, Farkas O, Tomasi J, Barone V, Cossi M, Cammi R, Mennucci B, Pomelli C, Adamo C, Clifford S, Ochterski J, Petersson GA, Ayala PY, Cui Q, Morokuma K, Salvador P, Dannenberg JJ, Malick DK, Rabuck AD, Raghavachari K, Foresman JB, Cioslowski J, Ortiz JV, Baboul AG, Stefanov BB, Liu G, Liashenko A, Piskorz P, Komaromi I, Gomperts R, Martin RL, Fox DJ, Keith T, Al-Laham MA, Peng CY, Nanayakkara A, Challacombe M, Gill PMW, Johnson B, Chen W, Wong MW, Andres JL, Gonzalez C, Head-Gordon M, Replogle ES, Pople JA. Gaussian 98, Revision A.11. Gaussian Inc: Pittsburgh PA, 2001; (b) Foresman JB, Frisch A. *Exploring Chemistry with Electronic Structure Methods*. Gaussian Inc: Pittsburgh PA, 1993.
15. Glendening ED, Reed AE, Carpenter JE, Weinhold F. *Gaussian NBO* Version 3.1.
16. van Duijneveldt FB, van Duijneveldt-van de Rijdt JGCM, van Lenthe JH. *Chem. Rev.* 1994; **94**: 1873–1885.
17. Mayer I, Surján PR. *Chem. Phys. Lett.* 1992; **191**: 497–499.
18. Emsley J, Hoyte OPA, Overill RE. *J. Am. Chem. Soc.* 1978; **100**: 3303–3306.
19. Salvador P, Duran M. *J. Chem. Phys.* 1999; **111**: 4460–4465.
20. Simon S, Duran M, Dannenberg JJ. *J. Chem Phys.* 1996; **105**: 11024–11031.
21. Papousek D, Aliev MR. *Molecular Vibrational-Rotational Spectra.* Elsevier: Amsterdam, 1982.
22. (a) Scott AP, Radom L. *J. Phys. Chem.* 1996; **100**: 16502–16513; (b) Wong MW. *Chem. Phys. Lett.* 1996; **256**: 391–399; (c) Pople JA, Scott AP, Wong MW, Radom L. *Israel J. Chem.* 1993; **33**: 345–350.
23. Loncharich RJ, Schwartz TR, Houk KN. *J. Am. Chem. Soc.* 1987; **109**: 14–23.
24. Salvador P, Béla P, Duran M, Suhai S. *J. Comp. Chem.* 2001; **22**: 756–786.
25. Vogt J, Mez-Starck B, Vogt N, Hutter W. *J. Mol. Struct*. 1999; **485–486**: 249–254.
26. Iijima K, Shibata S. *Bull. Chem. Soc. Jpn* 1979; **52**: 711–715.
27. Iijima K, Yamada T, Shibata S. *J. Mol Struct.* 1981; **77**: 271.
28. Jensen F. *Introduction to Computational Chemistry.* Wiley: New York, 1999; 265.
29. Tsuzuki S, Lüthi HP. *J. Chem. Phys.* 2001; **114**: 3949–3957.
30. Everaert GP, Herrebout WA, van der Veken BJ. *J. Phys. Chem. A* 2001; **105**: 9058–9067.
31. Cabaleiro-Lago EM, Ríos M. *Chem. Phys. Lett.* 1998; **294**: 272–276.
32. Reed AE, Weinstock RB, Weinhold F. *J. Chem. Phys.* 1985; **83**: 735–746.

